Efficient Protein-Ligand Binding Free Energy Estimation with Coarse-Grained Funnel Metadynamics

Andrea Grazzi,[†] Chelsea M. Brown,[‡] Maurizio Sironi,[†] Siewert J. Marrink,[*,‡] and Stefano Pieraccini[*,†]

†*Department of Chemistry, University of Milan, Via C. Golgi 19, 20133 Milan, Italy*

‡*Groningen Biomolecular Sciences and Biotechnology Institute, University of Groningen, Nijenborgh 7, 9747 AG, Groningen, The Netherlands*

E-mail: s.j.marrink@rug.nl; stefano.pieraccini@unimi.it

Abstract

Despite considerable advances in computational chemistry, bridging the gap between the accuracy of all-atom molecular dynamics (AA-MD) and the high-throughput capabilities of docking remains an unsolved problem in protein-ligand binding free energy predictions. In this work, we propose to address this challenge through coarse-grained funnel metadynamics (CG-FMD) with the Martini 3 forcefield. This approach combines the reduced computational cost of a CG representation with state-of-the-art enhanced sampling techniques and the interpretability of a physics-based forcefield. Specifically, the binding of colchicine to two different protein targets was modeled at both AA and CG resolutions, and the corresponding ΔG_{bind} predictions were compared with experimental references. Additionally, the robustness of CG-FMD-based ΔG_{bind} predictions was evaluated with respect to various aspects of the simulation setup by collecting more than 7 milliseconds of CG-FMD simulations. The results demonstrate that CG-FMD yields ΔG_{bind} estimates comparable to experimental values while requiring only a fraction of the computational cost of AA-MD simulations. Moreover, the extensive sampling achievable with CG-FMD reduces statistical uncertainty in the final predictions, effectively compensating for the simplified system representation. Future work should build upon these methodological insights to broaden the scope of ligands and targets explored.

Introduction

Accurate computation of protein-ligand binding affinities has long been an area of active interest in computational chemistry, as it can guide the drug design process by identifying novel potent compounds and help rationalize their mode of action. Classical high-throughput docking can screen many ligands cheaply, but its scoring functions are often oversimplified. In contrast, molecular dynamics (MD)–based free-energy methods explicitly include protein flexibility and solvent effects, potentially yielding more reliable affinities. To this end, many simulation strategies have been devised,[1] ranging from alchemical free-energy perturbation methods, where statistical mechanics is applied to compute the free energy differences between states connecting along a thermodynamics path bound and unbound endpoints, to physical pathway methods, where the entire ligand binding process is simulated. Metadynamics[2,3] is a well-established technique for enhancing the crossing of energy barriers and facilitating the sampling of rare events, a common challenge in the study of protein–ligand binding. In particular, a history dependent potential is deposited along the slow degrees of freedom of the system, named collective variables (CVs). This allows to accelerate the sampling and to recover the free energy surface (FES) of the system. Among the various metadynamics implementations, funnel metadynamics (FMD)[4] has emerged in recent years as a powerful tool for the identification of ligand binding free energy and binding pose. FMD applies a funnel shaped potential throughout the simulation, allowing for freedom of exploration inside the protein's pocket of interest while restricting the ligand roto-translation to a narrow cylinder outside the binding site, preventing dispersion in the solution bulk, which would be computationally inefficient. However, this approach suffers from the drawback typically associated with fully atomistic simulations, namely the challenge in scalability of the system size. In particular, proper sampling of the ligand unbound states requires an extensive solvation layer of the protein, which for larger biological targets can become computationally demanding, especially during the screening phase of the drug discovery process. An effective strategy for reducing the system size is offered by coarse-grained (CG) MD. A

CG forcefield simplifies the system representation by grouping several atoms into a smaller number of interaction sites called beads, using mapping schemes typically designed to maintain specificity at the level of chemical fragments. In particular, the Martini 3 forcefield[5] has emerged as a promising candidate for investigating protein-ligand interactions. Simulation of protein ligand binding have been successfully applied both to soluble[6–8] and transmembrane biosystems[9–12] . Performing MD simulations with the Martini 3 forcefield requires the investigator to carefully plan the simulation setup. For instance, in order to maintain elements of secondary and tertiary structure in the proteins, a set of additional bonded terms among backbone beads is required.[13,14] Many strategies have been devised over the years, ranging from a set of elastic restraints derived from a reference structure (i.e. Elastic Network, EN[15]) to more flexible models that rely on Gō-like bonds, such as OLIVES[16] and goMartini[17,18] models. The purpose of this investigation is to assess the feasibility of estimating ligand binding free energies with the Martini 3 forcefield by applying FMD. As a chemical probe, the compound colchicine, which is commonly used to modulate microtubule activity[19] and to treat inflammatory diseases,[20] will be applied to two different biological targets, namely BRD4 and Colchicalin. The first target, BRD4, is a member of the bromodomains (BRDs) family, responsible for recognition of the histone code and the regulation of gene expression.[21] The second target protein, Colchicalin, is a derivative of human lipocalin 2 designed to bind colchicine with picomolar affinity.[22] Binding free energy estimates obtained with CG-FMD will be compared with all-atom (AA) FMD and with experimental references for the two target systems. Furthermore, several aspects of the simulation protocol for CG-FMD will be extensively investigated. The influence of protein flexibility on binding estimate will be explored by applying the three models (i.e. EN, OLIVES, goMartini) to the backbone of the CG proteins. In addition, the effects on binding free energy prediction of the ligand parameterization and its dependence on the size of the funnel-shaped potential applied will be assessed. Overall, we aim to provide methodological insights useful for the extension of CG-FMD simulation approach to other cases of study, and eventually, an automated

computational pipeline for rational drug design.

Methods

Ligand parameterization

The atomistic structure of colchicine has been retrieved from the RCSB databank[23] and converted to CHARMM36-FF topology using the CGENFF python script.[24,25] Bonded terms for the CG-model of the ligand have been defined according to Martini 3 guidelines[26] based on structural behaviour from reference atomistic trajectory. To this end, the compound has been solvated with 4500 TIP3 water molecules, energy minimized with the steepest descent algorithm, equilibrated for 10 ns at 300 K (V-rescale thermostat,[27] τ_{T}=0.1 ps) and 1 bar pressure (Berendsen barostat, τ_{P}=5.0 ps , compressibility of $4.5 \cdot 10^{-5}$ bar^{-1}) and simulated for 1.050 μs with the Parrinello-Rahman barostat[28] (the first 50 ns have been considered as equilibration with the second barostat). This atomistic trajectory has been converted to CG-resolution using an AA to CG mapping (Figure S1A) and the center of geometry (COG) approach.[5,26] Validation of CG-bonded terms has been performed by inspecting overlap with the target AA-derived distribution (Figure S3). Global structural properties have been validated by computing the relative error on the difference of the solvent accessible surface area (SASA) between AA and CG simulations (Figure S4) and the Connoly-surface (Figure S5). The chemical behaviour of the CG model of the ligand is determined by the Martini 3 types attributed to its beads (Figure S1B). Validation of this type attribution scheme is performed by comparing the water-octanol partition coefficient of the CG ligand with available references[29] (Figure S2A). The logarithm of the water-octanol partition coefficient $\log P_{\mathrm{ow}}$ can be obtained by computing the desolvation free energy of the ligand in water and octanol as:

$$\log P_{\mathrm{ow}} = \frac{\Delta G_{\mathrm{oco}\rightarrow\mathrm{vac}} - \Delta G_{\mathrm{wat}\rightarrow\mathrm{vac}}}{\ln(10) RT} \tag{1}$$

where R is the ideal gas constant and T is the temperature of the simulated system (300 K). Desolvation free energies from water to vacuum ($\Delta G_{water \to vac}$) and from octanol ($\Delta G_{oco \to vac}$) to vacuum have been obtained through thermodynamic integration over ten windows of 60 ns (of which the first 10 ns have been discarded as equilibration). The error has been estimated as:

$$\epsilon_{\log \mathrm{P_{ow}}} = \frac{\sqrt{\epsilon^2_{\Delta G_{\mathrm{oco}\to\mathrm{vac}}} + \epsilon^2_{\Delta G_{\mathrm{wat}\to\mathrm{vac}}}}}{\ln(10) RT} \tag{2}$$

where each $\epsilon_{\Delta G}$ is the error associated with the desolvation free energy, as computed by `gmx bar`. Two ligand parameterizations have been considered: the first (henceforth referred to as "canonical") maximizes adherence to forcefield guidelines, the second (denominated "hydrophilic") maximizes the reproduction of the experimental $\log P_{\mathrm{ow}}$ value of colchicine (Figure S2B)

Protein Modelling

Atomistic parameters of the CHARMM-36m forcefield for BRD4 and Colchicalin protein have been generated with the CHARMM-GUI platform[30,31] starting from their crystallographic complex with colchicine (PDB ID 4LZR[32] and 5NKN,[22] respectively). Starting from the protein's pose, steepest descent minimization has been applied, followed by a 1 ns NVT equilibration with position restraints on C_α. Then, a multistep NPT equilibration with the Berendsen barostat has been applied to gradually release the position restraints (Table S1). For the production phase, three replicas of 500 ns AA-MD have been carried out with the apo proteins in the NPT ensemble with the Parrinello-Rahman barostat (τ_{P}=5.0 ps , compressibility of $4.5 \cdot 10^{-5}$ bar^{-1}) and the v-rescale thermostat (τ_{T}=1 ps). Backbone stability has been assessed through the computation of RMSD and RMSF with GROMACS tools. The suitability of CHARMM-36m forcefield for the investigation of the ligand-protein interaction has been assessed by performing AA-MD of the holo-complex. For consistency, the same equilibration protocol of the apo-protein has been applied to the holo-complex,

with the introduction of position restraints also on the heavy atom of the ligand, gradually released during the NPT equilibration (Table S1). Finally, production replicas of 200 ns each have been carried out in the NPT ensemble with the Parrinello-Rahman barostat and no position restraints. This protocol has been repeated six times for both colchicine-Colchicalin and colchicine-BRD4 complexes. Stability of the ligand crystallographic pose has been assessed through RMSD during production simulations over ligand's heavy atoms after trajectory fit to the protein's backbone (Figure S7). Backbone stability data from the AA-MD simulations has been employed to validate Martini 3 models of the two proteins. Generation of CG-structure file of the protein and Martini 3 parameters has been performed with martinize2 utility.[13] All three major tertiary network schemes have been generated and tested for both proteins. For the EN, an upper bond length of 0.8 nm (`martinize2 -eu 0.8`) has been requested and the elastic force constant has been defined as 750 kJ/mol. For OLIVES and goMartini, default settings have been maintained. After generation of the parameters, the CG-proteins have been solvated with water beads and NaCl has been included to neutralize the system's charge and reach a physiological concentration of 0.15 M. A minimization (steepest descent) and an equilibration in the NPT ensemble (Berendsen barostat, τ_P=4 ps, compressibility $3 \cdot 10^{-4}$ bar^{-1}) with position restraints on backbone beads for 50 ns at a timestep of 20 fs have been performed. Then, three production replicas of 2 μs have been collected for each protein model (EN, OLIVES, goMartini) with the Parrinello Rahman barostat (τ_P=12 ps, compressibility $3 \cdot 10^{-4}$ bar^{-1}). RMSD and RMSF of the CG-protein have been computed by considering the backbone beads and compared to the atomistic reference. For BRD4, three alternative goMartini parameterizations were tested by increasing the ϵ parameter of the Lennard-Jones potential by 15%, 25% and 50% respectively. This has allowed to reduce the RMSD instabilities and high RMSF observed in the standard implementation of goMartini (ϵ=9.414 kJ/mol) (Figure S10). In particular, the parameterization with ϵ=11.678 kJ/mol (ϵ_0+25%) provided a good compromise between reproduction of atomistic residue fluctuations, especially in the region surrounding the target

binding site (Figure S11), while still maintaining some degree of conformational flexibility. Therefore, this reparametrized ϵ value was selected as the reference for goMartini-BRD4.

Equilibrium CG-MD simulation

To perform equilibrium CG-MD simulations, Colchicalin and BRD4 have been solvated with water beads and NaCl has been added to a concentration of 0.15 M (Figure S12). Two ligand molecules have been added to each simulation box in random positions in the solvent bulk. For Colchicalin, all three protein models have been considered in combination with the canonical colchicine parameterization. The interaction of hydrophilic colchicine has been explored only with the EN-Colchicalin (Figure S13A). For BRD4, EN, OLIVES and an optimized goMartini network have been explored with the canonical ligand parameterization, while the hydrophilic colchicine has been used only for EN-BRD4 (Figure S13B). After initial minimization, NPT equilibration for 50 ns at 20 fs with Berendsen barostat has been performed. Fifteen independent production runs of 20.05 μs have been collected for each simulation setup with the Parrinello-Rahman barostat (τ_{P}=12 ps, compressibility $3 \cdot 10^{-4}$ bar^{-1}) (initial 50ns have been considered equilibration and disregarded from subsequent analysis). Neighbour-list settings have been modified according to the recommendations of Kim et al..[33] In particular, we set `verlet-buffer-tolerance=-1, rlist=1.35, nstlist=nsttcouple=nstpcouple=20`. Ligand occupancy isocurves have been computed with VMD.[34] A standard contact analysis approach has been applied with the `gmx mindist` tool to quantify the number of frames in which ligand molecules had non-zero contacts with the protein surface. The fraction $P_{bound} = \frac{\#Frames_{\mathrm{bound}}}{\#Simulation-frames}$ has been averaged across the independent replicas for each combination of ligand parameterization/protein model investigated (Table S2) to assess the influence of these aspects on the ligand's capability of exploring protein-bound states.

Atomistic FMD

The choice of the collective variable was guided by the objective of ensuring transferability to other case studies. A set of simple geometric descriptors of the ligand position with respect to the putative binding site has been defined. The first CV implemented is the distance between the center of mass (COM) of a group of residues constituting the binding site and the COM of the ligand. As a second CV, at first, we considered the dihedral angle between two residues and two points on the ligand scaffold. Later, we have extended the investigation to a hybrid-CV, consisting of dihedral character when the ligand is inside the pocket, while it assumes simple angular character for high distances. Details on the CV definition are provided in the Supporting Information (Figure S15, Figure S16, Figure S17). For the definition of the funnel-shaped restraining potential to be applied to the ligand, the FMAP-GUI has been used.[35] An upper restraint on the maximum distance between the ligand and the pocket of 2.8 nm has been imposed to allow exploration of well-solvated positions. An upper restraint on the global protein RMSD compared to the starting conformation of 0.3 nm (coherent with apo-protein flexibility, as shown in Figure S6) has been imposed to avoid excessive binding site rearrangements during ligand extraction under the metadynamics potential. Ligand starting conformation has been taken from holo simulations after 10 ns under NPT conditions. Initial set of simulations with the distance/dihedral CV set has been carried out with `biasfactor=30`, bias deposition rate every 1 ps, hills height of 2.0 kJ/mol and simulation duration of 300 ns. A second set of simulations with the distance/hybrid-CV set has been carried out with `biasfactor=12` and simulation length reduced to 200 ns. For every replica, a free energy surface (FES) has been computed after reweighting procedure. The binding constant, corrected by the presence of the funnel-shaped potential,[35] has been computed as:

$$K_b = C^0 \pi R_{cyl}^2 \int_{site} dz \exp(-\beta[W(z) - W_{ref}]) \tag{3}$$

Here, C^0 is the standard concentration equal to $1/1.661$ Å^{-3}, R_{cyl} is the radius of the cylinder towards the solvent, $W(z)$ is the value of the FES inside the basin of integration, W_{ref} is the free energy value in the unbound state and β is the inverse of the product between simulation temperature T and Boltzmann constant k_B. Basin boundaries for integration have been defined starting from the projection of the ligand crystallographic pose over the CV-space, as reported in Figure S16. The protein-ligand binding constant has been converted to a free energy value using the formula $\Delta G^0_{bind} = -k_B T \ln(K_b)$. Final binding affinity estimate for each simulation setup has been computed as average over the dataset with a statistical uncertainty given by the standard error of mean. An outlier removal criterion based on the modified Z-score has been applied when computing the average.

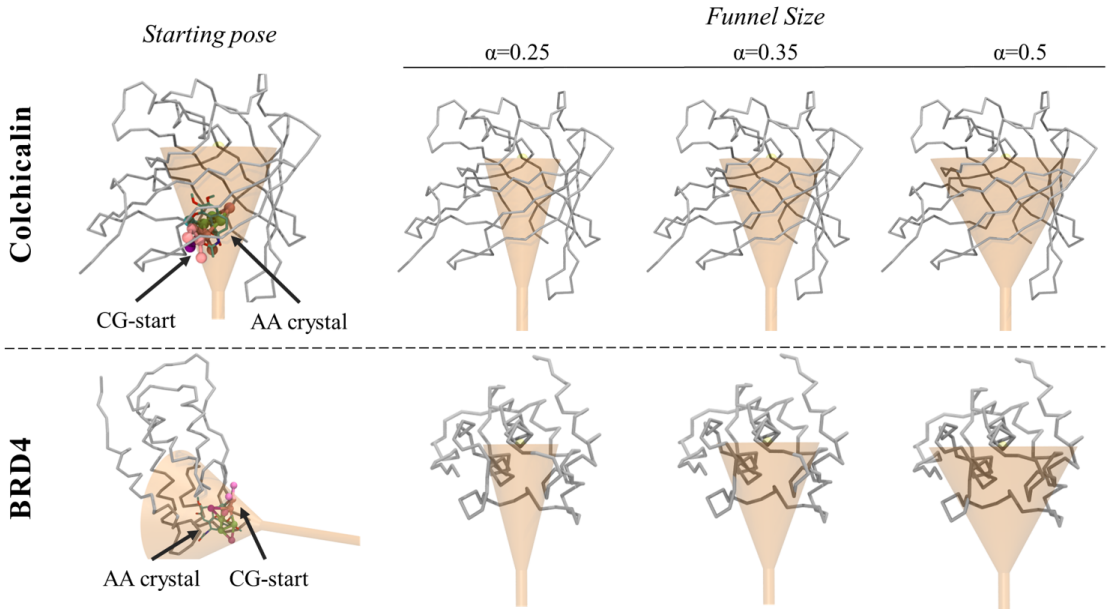

Figure 1: Funnel metadynamics (FMD) setup. The first column represents the overlap of the funnel-shaped position restraints applied to the COM of the ligand and the initial colchicine position for AA-FMD and CG-FMD. Starting pose for AA-FMD is represented in licorice, while CG-colchicine starting conformation is represented with ball & stick. Columns 2^{nd} to 4^{th} represent the three different funnel sizes investigated with CG-FMD by changing the angular aperture parameter α. The first row depicts the Colchicalin-colchicine system, while the second displays the BRD4 complex.

CG FMD

For every protein model, CG-FMD has been performed with both ligand parameterizations, to assess how much a significant difference in predicted CG-logP of 2 units affected the binding to the protein. In order to maintain comparability with atomistic results, the funnel-shaped potential has been oriented in the same way. The influence of the funnel size over the reproducibility of the affinity estimates has been assessed by repeating the simulations with three different funnel apertures (i.e. α=0.5 "Large", α=0.35 "Intermediate", α=0.25 "Small"). The choice of the collective variables has similarly been based on the same residues considered with AA-FMD. In this case, only a distance/angle combination has been used (Figure S15, Figure S16), given that applying a metadynamics potential to a dihedral angle with these CG-system yielded numerical instabilities regardless of the bias strength. Simulations have been repeated with two different bias strengths, namely a "mild" (`biasfactor=12`) and "strong" setup (`biasfactor=30`), to identify the best choice for convergence and reproducibility of results. For clarity, a graphical representation of the parameter space explored in the simulation setup is reported in Figure S19. Starting ligand conformation has been retrieved from equilibrium CGMD simulations, where the ligand has entered the pocket from the solvent bulk (Figure 1).

Assessment of simulation efficiency

To evaluate the simulation efficiency of CG-FMD compared to AA-FMD, the number of binding events observed across a subset of replicas of equal duration (1 μs) has been estimated for both the colchicine-Colchicalin and colchicine-BRD4 systems. In particular, the ligand has been annotated as bound whenever the distance ligand-pocket CV falls below a threshold of 5 Å. A smoothing procedure has been applied to account for oscillation of the CV around the threshold. In particular, if the time distance between two consecutive binding events was below a cooldown period ($t_{cooldown}$=1 ns), the two events have been merged. Furthermore, short-lived events ($t<min_{\text{duration}}$, with min_{duration}=2 ns) have been discarded. A rate of

binding events collection has been defined as $\lambda = \eta_{\text{events}}/t_{\text{wall}}$, where η_{events} is the average number of binding events observed in a simulation of 1 μs and t_{wall} is the wall time (in hours) necessary to complete the simulation of 1 μs. Further detail on the smoothing procedure and an evaluation of the robustness of the overall assessment for various values of t_{cooldown} and min_{duration} are provided in Figure S32 and Figure S33.

HPC Environment

AA-FMD simulations have been performed using GROMACS[36,37] 2022.3 patched with PLUMED[38,39] v2.8.1 on LEONARDO[40] Booster nodes (NVIDIA A100). CG-FMD and equilibrium CG-MD simulations have been carried out using GROMACS v2023.3 patched with PLUMED v2.9.0 on CPU-nodes of the Hábrók cluster, hosted by the Center for Information Technology of the University of Groningen. All other simulations have been performed using GROMACS v2023.5 on desktop workstations.

Results

Unbiased CG-MD simulation

The analysis of the ligand occupancy isocurves highlights how colchicine can access the experimentally known binding site starting from positions in the solvent bulk. In the case of Colchicalin, if we compare the volume of regions with the same isovalue, we can observe that it is higher for more flexible models (e.g. OLIVES and goMartini) compared to EN. The difference is even starker for the BRD4 system, where the occupancy inside the crystallographic site is limited to approximately 0.02 if an elastic network is applied to the protein, whereas it increases five-times to 0.10 if an OLIVES network is used. Interestingly, if we compare occupancies across the two proteins, we can observe that higher isovalues are observed for Colchicalin compared to BRD4, coherently with the difference in experimental affinity (Table 1). By comparing isosurfaces obtained with the two different ligand parameterizations

and the same protein model (EN), it is possible to observe how the identified pockets from equilibrium are topographically similar, but with a significant difference in terms of absolute occupancy values (Figure S14). In particular, the hydrophilic parameterization tends to spend a higher fraction of the simulation time in fully solvated states, exploring less frequently protein-bound configurations compared to the canonical parameterization (Table S2).

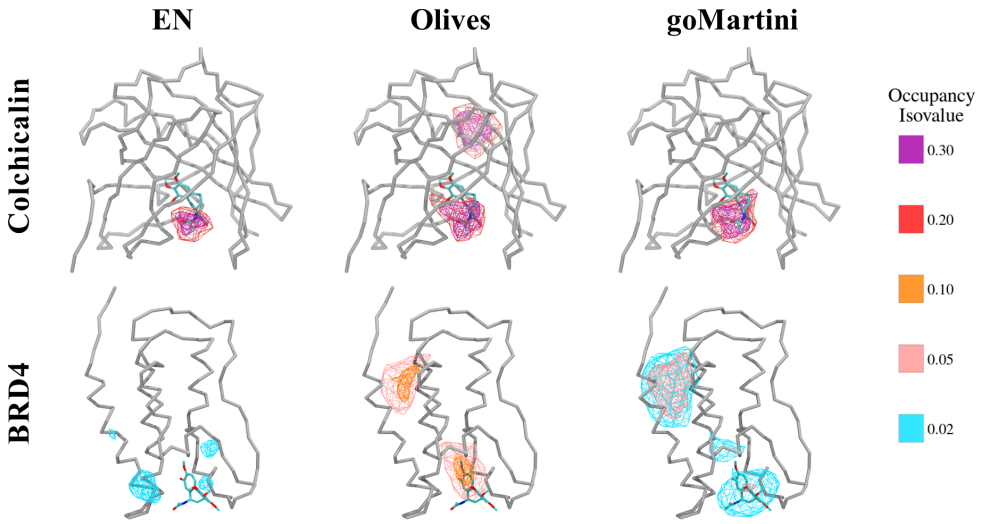

Figure 2: Influence of protein model on ligand occupancy isosurfaces from unbiased CG-MD simulations. The first row contains results for the three protein tertiary network schemes applied to Colchicalin. The second row contains results for the two models applied to BRD4. Occupancies for the canonical colchicine parameterization are reported.

AA-FMD

Starting from a relaxed conformation of the ligand inside the crystallographic site, several independent replicas of AA-FMD have been carried out. Initially, a ligand-protein distance and dihedral angle have been used as CV pairs (Figure S15, Figure S16). The analysis of the FES shows a well-defined basin of minimum energy overlapping with the experimental pose for Colchicalin. In the case of BRD4, the basin is somewhat shallower. A second set of replicas has been collected for both protein systems using different sets of CVs. The ligand-protein distance has been maintained as the first CV, while a linear combination of ligand-protein angle and dihedral angle (Figure S17) was employed for the second CV. This

choice was based on the geometry of the funnel restraint that is applied to the ligand-protein system. Inside the pocket, the ligand is allowed to explore all orientations with respect to two protein residues (as defined by the dihedral angle). On the other hand, upon exit from the binding site, the CV becomes a simple angle between the ligand and the same two protein residues. Given that the funnel restraint for high distances is a narrow cylinder, which translates in a limited range of angular values that can be explored by the ligand, this allows quicker exploration of the solvated states. Interestingly, applying this hybrid CV allows to reduce the duration of each replica by one third while still recovering the same free energy landscape in both protein systems investigated (Figure S24). Binding free energy estimates for Colchicalin are -11.3±1.6 kcal/mol for the distance-dihedral CV set and -11.7±1.9 kcal/mol for the distance-hybrid CV pair, which are comparable to the experimental reference of -13.6 kcal/mol. In the case of BRD4, the affinity estimate is -8.5±1.2 kcal/mol for the distance-dihedral CV set and -8.8±1.0 kcal/mol for the distance-hybrid CV pair, presenting a difference of approximately 2 kcal/mol from the experimental reference of -6.4 kcal/mol. AA-FMD predictions are in very good agreement with experimental reference both for Colchicalin and BRD4 and the deviation from experimental value is comparable to recent works reported in literature,[41,42] as summarized in Figure S23.

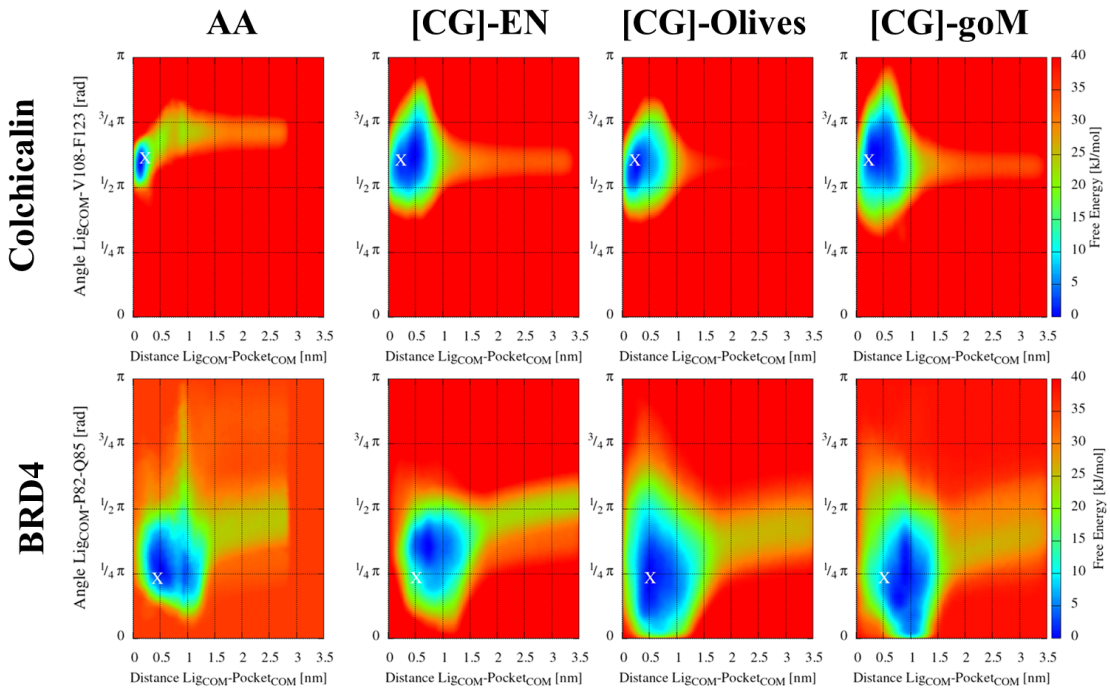

Figure 3: Comparison of FES obtained from FMD at different model resolution. The first column contains data from AA simulations, while columns 2^{nd} to 4^{th} reports results from CG-FMD simulations with different protein network models. The first row refers to the Colchicalin-colchicine complex, while the second-row present results for the colchicine-BRD4 complex. For atomistic data, the FES has been obtained with the distance-hybridCV CV-pair. For CG-results, only the FES obtained with intermediate funnel size ($\alpha = 0.35$), mild bias strength (`biasfactor=12`) and canonical ligand parameterization are presented.

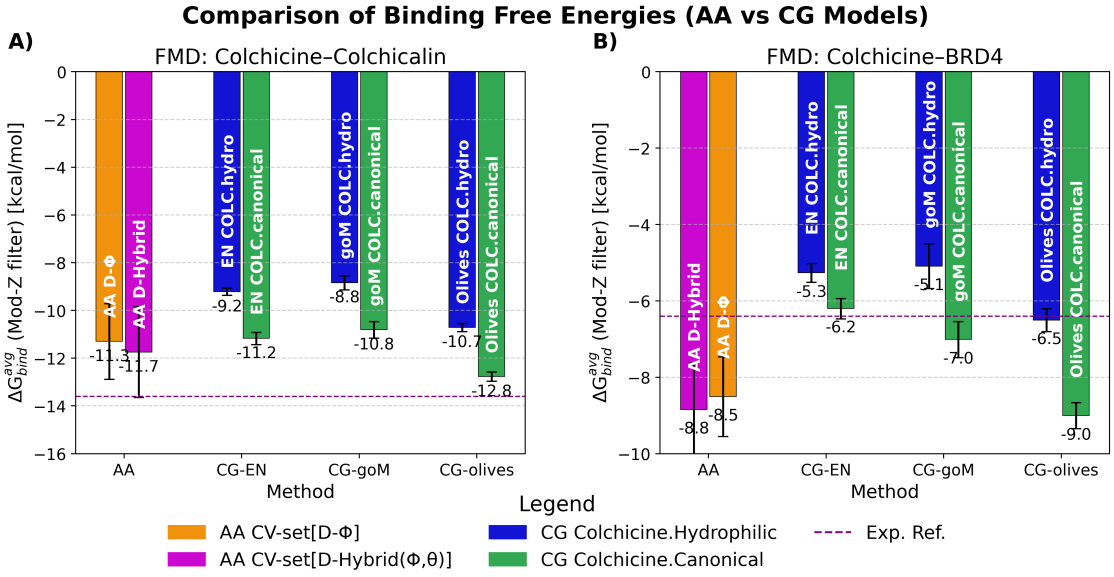

Figure 4: Colchicine binding free energy estimated from FMD. On the left, results for the colchicine-Colchicalin complex. On the right, results for the colchicine-BRD4 complex. Orange and pink bars represent AA-FMD values obtained with the distance-dihedral / distance-hybridCV CV sets respectively. Blue and green bars symbolise CG-FMD estimates obtained with the hydrophilic/canonical ligand parameterization of CG-colchicine across different protein backbone networks (x-axis groups). Pink dashed line indicates experimental reference.

Table 1: Comparison of experimental colchicine binding free energy with computational estimates obtained with FMD at AA and CG resolution. Last column reports the absolute value of the difference between the experimental reference and the FMD estimate. For CG-FMD, only results obtained with the canonical colchicine parameterization have been included.

Protein	Ligand	Type	ΔG_{bind} [kcal/mol]	$\lvert\Delta\Delta G^{exp-FMD}_{bind}\rvert$ [kcal/mol]
BRD4	Colchicine	Experimental[a]	-6.4	-
BRD4	Colchicine	AA-FMD	-8.8 ± 1.2	2.4
BRD4	Colchicine	AA-FMD	-8.5 ± 1.0	2.1
BRD4	Colchicine	CG-FMD (EN)	-6.2 ± 0.2	0.2
BRD4	Colchicine	CG-FMD (goMartini)	-7.0 ± 0.5	0.6
BRD4	Colchicine	CG-FMD (OLIVES)	-9.0 ± 0.3	2.6
Colchicalin	Colchicine	Experimental[b]	-13.6	-
Colchicalin	Colchicine	AA-FMD	-11.3 ± 1.6	2.3
Colchicalin	Colchicine	AA-FMD	-11.7 ± 1.9	1.9
Colchicalin	Colchicine	CG-FMD (EN)	-11.2 ± 0.3	2.4
Colchicalin	Colchicine	CG-FMD (goMartini)	-10.8 ± 0.3	2.8
Colchicalin	Colchicine	CG-FMD (OLIVES)	-12.8 ± 0.3	0.8

[a] Lucas et al.[32] [b] Barkovskiy et al.[22]

CG-FMD

To assess the reproducibility of the ligand binding free energy estimates with CG-FMD, we have collected several sets of simulations with different combinations of protein network, funnel size and metadynamics `biasfactor`, as reported in Figure S20 and Figure S21. In the case of Colchicalin, CG estimates for the ligand canonical parameterization and the EN or goMartini model, -11.2±0.3 kcal/mol and -10.8±0.3 kcal/mol, are comparable with the -11.3±1.6 kcal/mol obtained through AA-FMD and the experimental reference of -13.6 kcal/mol. Allowing more flexibility to the binding site with the application of the OLIVES network increases the CG-FMD estimate to -12.8±0.3. Interestingly, by repeating the simulations with a more hydrophilic ligand parameterization, we observe a decrease in the binding free energy of approximately 2 kcal/mol across all protein models. This is consistent with the observation already drawn from equilibrium CG-MD, where the ligand occupancy of the binding site was significantly reduced and colchicine spent a larger share of the simulation time in the unbound state compared to the canonical parameterization. When considering the BRD4 protein system, CG-FMD estimate for the canonical colchicine parameterization and the EN protein network is -6.2±0.2 kcal/mol, which is remarkably close to the experimental reference of -6.4 kcal/mol. As seen for the case of Colchicalin, introducing a more flexible backbone model such as goMartini or OLIVES increases the CG binding estimate to -7.0±0.5 and -9.0±0.3 kcal/mol respectively, which is still comparable with the prediction of -8.5±1.0 kcal/mol obtained from AA-FMD. A notable feature is the rapid convergence observed in the binding affinity estimates. In particular, if we consider the evolution of the average binding free energy across the set of ten replicas per simulation setup, we can observe how the average typically converges after three to four microseconds for simulations collected with a mild bias (`biasfactor=12`), both for Colchicalin (Figure 5) and BRD4 (Figure 6). Simulations collected with a stronger bias (`biasfactor=30`) reassuringly converge to similar values but may present initially higher oscillations in the average estimate. Furthermore, we note on passing that the combination of a narrow funnel and strong bias setup led to

numerical instabilities, preventing some replicas from reaching the target duration of 10 μs. Concerning the influence of the size of the funnel-shaped potential on the CG-FMD prediction, it is interesting to observe that the estimates vary across a span typically below 0.4 kcal/mol (Figure S25 and Figure S26), which is comparable to the uncertainty associated with each average. Thus, data suggests that the funnel shape has no significant influence on the computed binding free energy.

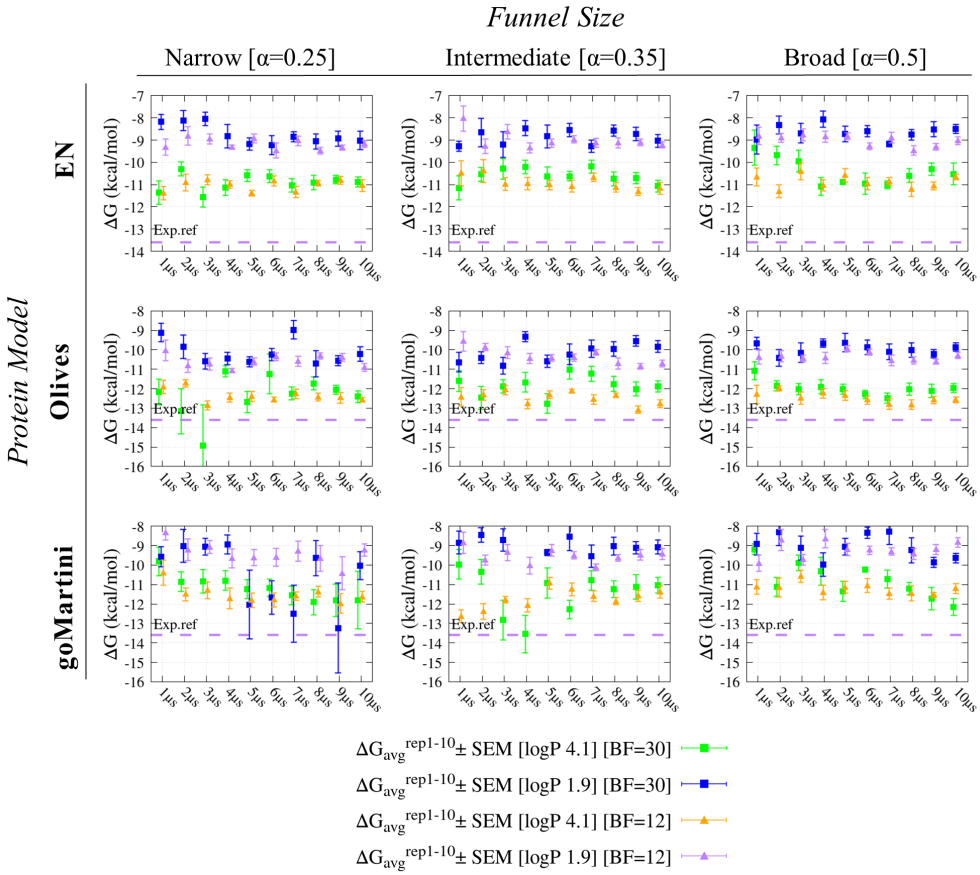

Figure 5: Convergence of colchicine-Colchicalin binding free energy. Square-shaped data points represent results obtained with a stronger bias (`biasfactor=30`) and canonical (green) or hydrophilic (blue) ligand parameterization. Triangular points signify results obtained with a mild bias (`biasfactor=12` and canonical (orange) or hydrophilic (purple) ligand parameterization. Purple dashed line indicates the experimental affinity reference.

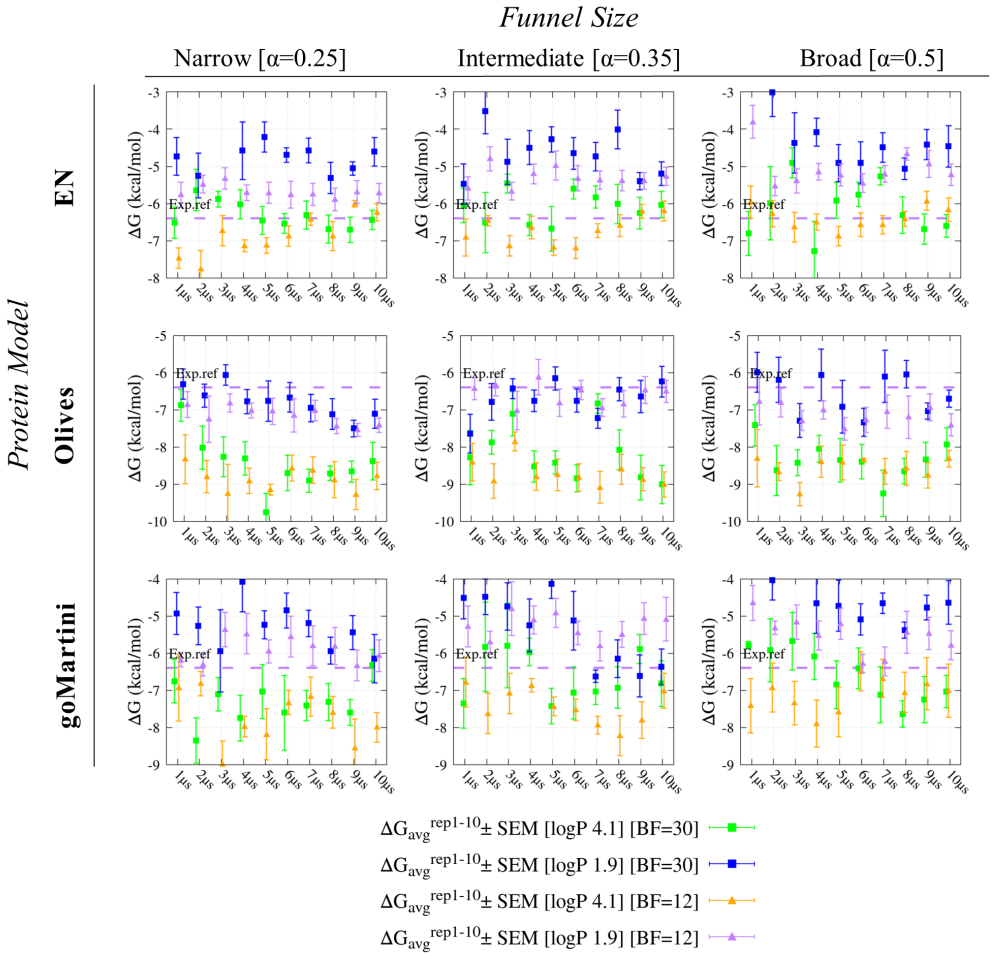

Figure 6: Convergence of colchicine-BRD4 binding free energy. Square-shaped data points represent results obtained with a stronger bias (`biasfactor=30`) and canonical (green) or hydrophilic (blue) ligand parameterization. Triangular points signify results obtained with a mild bias (`biasfactor=12` and canonical (orange) or hydrophilic (purple) ligand parameterization. Purple dashed line indicates the experimental affinity reference.

Convergence of binding free energy estimates

Convergence of free energy estimates obtained from enhanced sampling techniques presents some critical aspects well-documented in the literature. For instance, Aho et al. [43] observed that differences for umbrella sampling (US) replicas may oscillate in an interval of 2-20 kcal/mol. By gradually reducing the bias deposited as the simulation progresses, well-tempered metadynamics has been demonstrated to asymptotically converge. [44] However, the choice of CVs is critical in achieving good convergence. Indeed, many guidelines are available [45] and alternative simulation protocols have been devised to compensate for the choice of suboptimal CV sets. [46] The purpose of this work is to assess the solidity of CG-FMD, therefore we opted for simple geometric descriptors of our systems as CVs, considering that they could be easily extended to other cases of studies. As statistical uncertainty for the binding affinity estimates, we have considered the SEM across collection of independent replicas. Comparing the order of magnitude of this error for atomistic and Martini 3 systems yields interesting insights. As reported in Table 1, the uncertainty associated with AA-FMD results in this work is typically greater than 1 kcal/mol. This is quite striking, especially considering that significant number of replicas have been collected, ranging from sixteen to twenty (Figure S22). Figure S27 provides greater detail on the free energy prediction evolution for each independent replica of the colchicine-Colchicalin case with the distance/dihedral angle CV set. Interestingly, all replicas show that within 300 ns the bias added has decreased to negligible values, but while some simulations have converged to a value close to the experimental reference, others present a different trend. To assess whether longer simulation time could improve convergence, the simulation duration has been increased to 1 μs for three replicas of both proteins. Figure S28 and Figure S29 show that, for both systems, while two simulations oscillate in the proximity of the reference value (replicas 2,3 in Figure S28, replicas 2,3 in Figure S29), a third still fails to properly reach convergence. This can be rationalized by recognizing that our geometric CVs do not fully capture all the relevant slow degrees of freedom of the system. Interestingly, if we compare the evolution

of the average binding free energy over short time for twenty replicas with the average over longer times for three replicas, we can observe that they oscillate around similar values, but the statistical uncertainty associated with the smaller dataset is definitely higher. It would seem reasonable therefore to suggest that performing several replicas on shorter timescales is better compared to focusing on few quite long simulations. In contrast, CG-FMD presents remarkably good convergence properties. The SEM associated with the average free energy over datasets of ten replicas is typically below 0.4 kcal/mol, as reported in Table 1. Furthermore, the convergence of the individual simulations is achieved typically within two to three microseconds, as shown in Figure S30 for a setup with a slowly decreasing metadynamics bias (`biasfactor=30`) and Figure S31 for a milder bias (`biasfactor=12`). A comparison of the computational efficiency in sampling binding phenomena was performed by computing the average number of binding events observed in simulation of equal duration (1 μs) both at AA and CG level. As reported in Table 2, if we consider the wall time duration, CG-FMD simulations have collected binding events at a rate λ that is ten times faster compared to AA-FMD for the colchicine-(EN)BRD4 complex, while is twenty five times faster for the colchicine-(EN)Colchicalin case. Additional λ^{CG} estimates for the other protein models considered are reported in Figure S33. Moreover, the substantially lower hardware demands of CG simulations enable far greater scalability, broadening the scope of feasible investigations.

Table 2: Benchmark of the performances obtained for AA-FMD and CG-FMD. Results obtained using a $t_{cooldown}$=1 ns and t<min_{duration}=2 ns in the binding events counting protocol. More data on the robustness of this estimate using other parameters is reported in the SI.

Simulation type	CPU-allocation	GPU	Protein	Performance [ns/day]	Walltime [h]	$\eta_{1\mu s}$ [Events]	λ [Events/h]
AA-FMD	8-cores[a]	1[c]	Colchicalin	190	126.3	14.3	0.11
CG-FMD	8-cores[b]	*none*	(EN)Colchicalin	3600	6.7	18.9	2.63
AA-FMD	8-cores[a]	1[c]	BRD4	190	126.3	28.3	0.22
CG-FMD	8-cores[b]	*none*	(EN)BRD4	3600	6.7	17.6	2.63

[a] Intel Xeon Platinum 8358@2.60GHz [b] AMD EPYC 7763@2.45 GHz [c] NVIDIA Ampere A100 64GB

Conclusions

In this study, we combined FMD with the Martini 3 forcefield to estimate protein-ligand binding free energies from CG-MD simulations. We found that CG-FMD simulations yield binding affinity predictions comparable in accuracy to AA-FMD counterparts at a fraction of the computational cost. Furthermore, we observed that convergence is easily obtained at CG resolution, thanks to the increased sampling that can be readily collected. The significant reduction in statistical uncertainty observed with Martini 3 simulations compensates for the simplified description of the system, compared to a more accurate fully atomistic resolution. The robustness of the CG-FMD protocol has been assessed by exploring several simulation setups. Reassuringly, we found that CG binding free energy prediction does not vary significantly by changing the size of the funnel or the rate of decrease in the metadynamics bias. In addition, we observed that allowing more flexibility in the protein by implementing an OLIVES network compared to an Elastic Network yields a stronger binding affinity estimate. While this work has been focused on a single ligand binding to two different protein targets, future studies should investigate the capability of CG-FMD to rank affinity of different chemical scaffolds for the same binding site, thereby assessing the level of chemical accuracy that can be achieved with the Martini 3 forcefield.[6] With the rise of new tools for streamlining the parametrization of novel ligands to CG-resolution[47],[48] the combination of FMD with the Martini 3 forcefield could offer an alternative, cost-effective, physics-based method to estimate binding affinities of drug-candidates to biological targets, with high scalability of system size and complexity.

Acknowledgement

We thank the Center for Information Technology of the University of Groningen for their support and for providing access to the Hábrók high performance computing cluster. We acknowledge ISCRA for awarding this project access to the LEONARDO supercomputer,

owned by the EuroHPC Joint Undertaking, hosted by CINECA (Italy). This research was supported by the University of Milan (PSR 2023 Linea 2).

Supporting Information Available

Supporting Information: validation of ligand parameterization, additional data on proteins' modelling, details on equilibium CG-MD setup, additional data on AA-FMD and CG-FMD, assessment of simulation efficiency (PDF) Supplementary material, including the Martini 3 parameters for the protein and ligand investigated in this work, as well as the starting simulation box for CG-FMD, is provided as a compressed folder (ZIP).

References

(1) Limongelli, V. Ligand binding free energy and kinetics calculation in 2020. *Wiley Interdisciplinary Reviews Computational Molecular Science* **2020**, *10*.

(2) Laio, A.; Parrinello, M. Escaping free-energy minima. *Proceedings of the National Academy of Sciences* **2002**, *99*, 12562–12566.

(3) Barducci, A.; Bonomi, M.; Parrinello, M. Metadynamics. *Wiley Interdisciplinary Reviews Computational Molecular Science* **2011**, *1*, 826–843.

(4) Limongelli, V.; Bonomi, M.; Parrinello, M. Funnel metadynamics as accurate binding free-energy method. *Proceedings of the National Academy of Sciences* **2013**, *1*, 6358–6363.

(5) Souza, P. et al. Martini 3: a general purpose force field for coarse-grained molecular dynamics. *Nature Methods* **2021**, *18*, 382–388.

(6) Souza, P.; Thallmair, S.; Conflitti, P.; Ramírez-Palacios, C.; Alessandri, R.; Raniolo, S.;

Limongelli, v.; Marrink, S. J. Protein–ligand binding with the coarse-grained Martini model. *Nature Communications* **2020**, *11*, 3714.

(7) Davoudi, S.; Vainikka, P. A.; Marrink, S. J.; Ghysels, A. Validation of a Coarse-Grained Martini 3 Model for Molecular Oxygen. *Journal of Chemical Theory and Computation* **2024**, *21*.

(8) Nemchinova, M.; Schuurman-Wolters, G. K.; Whittaker, J. J.; Arkhipova, V.; Marrink, S. J.; Poolman, B.; Guskov, A. Exploring the Ligand Binding and Conformational Dynamics of the Substrate-Binding Domain 1 of the ABC Transporter GlnPQ. *The Journal of Physical Chemistry B* **2024**, *128*, 7822–7832.

(9) Bartocci, A.; Grazzi, A.; Awad, N.; Corringer, P.-J.; Souza, P. C. T.; Cecchini, M. A millisecond coarse-grained simulation approach to decipher allosteric cannabinoid binding at the glycine receptor α1. *Nature Communications* **2024**, *15*, 9040.

(10) Bieker, S.; Timme, M.; Woge, N.; Hassan, D. G.; Brown, C. M.; Marrink, S. J.; Melo, M. N.; Holthuis, J. C. M. Hexokinase-I directly binds to a charged membrane-buried glutamate of mitochondrial VDAC1 and VDAC2. *Communications Biology* **2025**, *8*, 212.

(11) Diamanti, E.; Souza, P.; Setyawati, I.; Bousis, S.; Monjas, L.; Swier, L.; Shams, A.; Tsarenko, A.; Stanek, W.; Jäger, M.; Marrink, S.; Slotboom, D.; Hirschs, A. Identification of inhibitors targeting the energy-coupling factor (ECF) transporters. *Communications Biology* **2023**, *6*, 1182.

(12) Waclawiková, B.; Souza, P.; Schwalbe, M.; Neochoritis, C.; W.H., S.; A., N.; Marrink, S. J.; S., E. A. Potential binding modes of the gut bacterial metabolite, 5-hydroxyindole, to the intestinal L-type calcium channels and its impact on the microbiota in rats. *Gut Microbes* **2022**, *15*, 2154544.

(13) Kroon, P. C.; Grunewald, F.; Barnoud, J.; Tilburg, M. v.; Brasnett, C.; Telles, C.; Wassenaar, T. A.; Marrink, S. Martinize2 and Vermouth: Unified Framework for Topology Generation. *eLife* **2023**, *12*, RP90627.

(14) Borges-Araújo, L.; Pereira, G.; Valério, M.; Souza, P. Assessing the Martini 3 protein model: A review of its path and potential. *Biochimica Et Biophysica Acta (BBA)* **2024**, *1872*, 141014.

(15) Periole, X.; Cavalli, M.; Marrink, S.; A., C. M. Combining an elastic network with a Coarse-Grained molecular force field: structure, dynamics, and intermolecular recognition. *Journal of Chemical Theory and Computation* **2009**, *5*, 2531–2543.

(16) Pedersen, K. B.; Borges-Araújo, L. A.; Souza, P. C.; Marrink, S. J.; SchiØtt, B. OLIVES: a G$\bar{O}$-like model for stabilizing protein structure via hydrogen bonding native contacts in the Martini 3 Coarse-Grained Force Field. *Journal of Chemical Theory and Computation* **2024**, *20*, 8049–8070.

(17) Poma, A. B.; Cieplak, M.; Theodorakis, P. E. Combining the MARTINI and Structure-Based Coarse-Grained approaches for the molecular dynamics studies of conformational transitions in proteins. *Journal of Chemical Theory and Computation* **2017**, *13*, 1366–1374.

(18) Souza, P. C. T. et al. GōMartini 3: From large conformational changes in proteins to environmental bias corrections. *Nature Communications* **2025b**, *16*, 4051.

(19) Weisenberg, R. C. Colchicine-binding protein of mammalian brain and its relation to microtubules. *Biochemistry* **2025b**, *7*, 4466–4479.

(20) Niel, E.; Scherrmann, J. Colchicine today. *Joint Bone Spine* **2025b**, *73*, 672–678.

(21) Muller, S.; Filippakopoulos, P.; Knapp, S. Bromodomains as therapeutic targets. Expert Reviews in Molecular Medicine. *Expert Reviews in Molecular Medicine* **2011**, *13*.

(22) Barkovskiy, M.; Ilyukhina, E.; Dauner, M.; Eichinger, A.; Skerra, A. An engineered lipocalin that tightly complexes the plant poison colchicine for use as antidote and in bioanalytical applications. *Biological Chemistry* **2018**, *400*, 351–366.

(23) Berman, H.; Westbrook, J.; Feng, Z.; Gilliland, G.; Bhat, T.; Weissig, H.; Shindyalov, I.; Bourne, P. The Protein Data Bank. *Nucleic Acids Research* **2000**, *28*, 235–242.

(24) Vanommeslaeghe, K.; Hatcher, E.; Acharya, C.; Kundu, S.; Zhong, S.; Shim, J.; Darian, E.; Guvench, O.; Lopes, P.; Vorobyov, I.; Mackerell Jr., A. CHARMM general force field: A force field for drug-like molecules compatible with the CHARMM all-atom additive biological force fields. *Journal of Computational Chemistry* **2009**, *31*, 671–690.

(25) Vanommeslaeghe, K.; MacKerell Jr., A. D. Automation of the CHARMM General Force Field (CGENFF) i: bond perception and atom typing. *Journal of Chemical Information and Modeling* **2012**, *52*, 3144–3154.

(26) Alessandri, R.; Barnoud, J.; Gertsen, A.; Patmanidis, I.; de Vries, A. H.; Souza, P. C. T.; Marrink, S. J. Martini 3 Coarse-Grained Force Field: Small Molecules. *Advanced Theory and Simulations* **2021**, *5*, 2100391.

(27) Bussi, G.; Donadio, D.; Parrinello, M. Canonical sampling through velocity rescaling. *The Journal of Chemical Physics* **2007**, *126*, 014101.

(28) Parrinello, M.; Rahman, A. Polymorphic transitions in single crystals: A new molecular dynamics method. *Journal of Applied Physics* **1981**, *52*, 7182–7190.

(29) Ulrichová, J.; Walterová, D.; Lukič, V.; Černochová, D.; Chromcová, I.; Šimánek, V. Biochemical evaluation of colchicine and related analogs. *Planta Medica* **1981**, *59*, 144–147.

(30) Jo, S.; Kim, T.; Iyer, V. G.; Im, W. CHARMM-GUI: A web-based graphical user interface for CHARMM. *Journal of Computational Chemistry* **2008**, *29*, 1859–1865.

(31) Lee, J. et al. CHARMM-GUI Input Generator for NAMD, GROMACS, AMBER, OpenMM, and CHARMM/OpenMM simulations using the CHARMM36 Additive Force Field. *Journal of Chemical Theory and Computation* **2015b**, *12*, 405–413.

(32) Lucas, X.; Wohlwend, D.; Hügle, M.; Schmidtkunz, K.; Gerhardt, S.; Schüle, R.; Jung, M.; Einsle, O.; Günther, S. 4-Acyl Pyrroles: Mimicking Acetylated lysines in Histone Code Reading. *Angewandte Chemie International Edition* **2013**, *52*, 14055–14059.

(33) Kim, H.; Fábián, B.; Hummer, G. Neighbor list artifacts in molecular Dynamics simulations. *Journal of Chemical Theory and Computation* **2023**, *19*, 8919–8929.

(34) Humphrey, W.; Dalke, A.; Schulten, K. VMD - Visual Molecular Dynamics. *Journal of Molecular Graphics* **1996**, *14*, 33–38.

(35) Raniolo, S.; Limongelli, V. Ligand binding free-energy calculations with funnel metadynamics. *Nature Protocols* **2020b**, *15*, 2837–2866.

(36) Berendsen, H.; Van Der Spoel, D.; Van Drunen, R. GROMACS: A message-passing parallel molecular dynamics implementation. *Computer Physics Communications* **1995**, *91*, 43–56.

(37) Abraham, M. J.; Murtola, T.; Schulz, R.; Páll, S.; Smith, J. C.; Hess, B.; Lindahl, E. GROMACS: High performance molecular simulations through multi-level parallelism from laptops to supercomputers. *SoftwareX* **2015**, *1-2*, 19–25.

(38) The PLUMED consortium Promoting transparency and reproducibility in enhanced molecular simulations. *Nature Methods* **2019**, *16*, 670–673.

(39) Tribello, G. A.; Bonomi, M.; Branduardi, D.; Camilloni, C.; Bussi, G. PLUMED 2: New feathers for an old bird. *Computer Physics Communications* **2013b**, *185*, 604–613.

(40) Turisini, M.; Cestari, M.; Amati, G. LEONARDO. A Pan-European Pre-Exascale Supercomputer for HPC and AI applications. *Journal of Large-scale Research Facilities JLSRF* **2024**, *9*.

(41) Swain, S.; Metya, A. K. Exploring Metformin's therapeutic Potential for Alzheimer's Disease: An In-Silico Perspective using Well-Tempered Funnel Metadynamics. *Journal of Chemical Theory and Computation* **2025**, *65*, 4163–4172.

(42) Rubina, N.; Moin, S. T. Attempting Well-Tempered Funnel metadynamics simulations for the evaluation of the binding kinetics of methionine Aminopeptidase-II inhibitors. *Journal of Chemical Information and Modeling* **2023**, *63*, 7729–7743.

(43) Aho, N.; Groenhof, G.; Buslaev, P. Do All Paths Lead to Rome? How Reliable is Umbrella Sampling Along a Single Path? *Journal of Chemical Theory and Computation* **2024**, *20*, 6674–6686.

(44) Dama, J. F.; Parrinello, M.; Voth, G. A. Well-Tempered metadynamics converges asymptotically. *Journal of Chemical Theory and Computation* **2012**, *112*, 240602.

(45) Valsson, O.; Tiwary, P.; Parrinello, M. Enhancing Important Fluctuations: Rare Events and Metadynamics from a Conceptual Viewpoint. *Annual Review of Physical Chemistry* **2016**, *67*, 159–184.

(46) Invernizzi, M.; Parrinello, M. Making the best of a bad situation: a multiscale approach to free energy calculation. *Journal of Chemical Theory and Computation* **2019**, *15*, 2187–2194.

(47) Pereira, G. P.; Alessandri, R.; Domínguez, M.; Araya-Osorio, R.; Grünewald, L.; Borges-Araújo, L.; Wu, S.; Marrink, S. J.; Souza, P. C. T.; Mera-Adasme, R. Bar-

tender: Martini 3 Bonded Terms via Quantum Mechanics-Based Molecular Dynamics. *Journal of Chemical Theory and Computation* **2024**, *20*, 5763–5773.

(48) Szczuka, M.; Pereira, G.; Walter, L.; Gueroult, M.; Poulain, P.; Bereau, T.; Souza, P.; Chavent, M. Fast parameterization of Martini3 models for fragments and small molecules. *bioRxiv* **2025**,

TOC Graphic

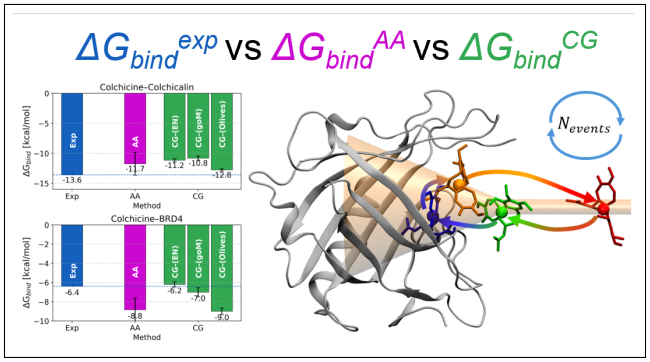
ΔG bind exp vs ΔG bind AA vs ΔG bind CG
Colchicine–Colchicalin
Exp
AA
CG-(EN)
CG-(goM)
CG-(Olives)
-13.6
-11.7
-11.2
-10.8
-12.6
Exp
AA
CG
Method
Colchicine–BRD4
-6.4
-6.2
-7.0
-7.0
N events